FUDMA Journal of Sciences (FJS)
ISSN online: 2616-1370
ISSN print: 2645 - 2944
Vol. 9 No. 4, April, 2025, pp 87 - 98
DOI: https://doi.org/10.33003/fjs-2025-0904-3274

EFFECT OF SCATTERER DISTRIBUTION ON RANDOM LASER MODEL USING OPTI-FDTD

***[1]Momoh Hameed Adavize and [2]Mohammed Ahmed**

[1]Department of Physics, Confluence University of Science and Technology, Osara, Kogi State, Nigeria
[2]Department of Physical Sciences, Niger State Polytechnic, Zungeru.

*Corresponding authors' email: adavizehameed@gmail.com

ABSTRACT
Random lasers, unlike conventional lasers, rely on multiple scattering in a disordered gain medium to achieve optical feedback, making scatterer distribution a crucial factor in their performance. This study investigates the effect of scatterer distribution on random laser performance using the Optical Finite-Difference Time-Domain (Opti-FDTD) simulation tool. The primary objective is to examine how varying scatterer densities—low, medium, and high—affect key lasing parameters, including lasing threshold, emission spectrum, and spatial coherence. Methodologically, the study involves designing photonic bandgap (PBG) structures, systematically varying scatterer arrangements, and analysing the resulting optical behaviours through simulation. Key findings indicate that medium-density scatterer configurations achieve the lowest lasing threshold and the most well-defined emission spectra, offering an optimal balance between light feedback and scattering losses. High-density distributions enhance spatial coherence due to stronger light localization but introduce higher thresholds and spectral overlap, while low-density configurations suffer from weak feedback and reduced performance metrics. The results align with theoretical predictions and experimental data, emphasizing the critical role of scatterer distribution in optimizing random laser designs. These insights hold significant implications for developing more efficient random lasers for applications in imaging, spectroscopy, sensing, and energy-efficient lighting.

Keywords: Scatterer Distribution, Random Lasers, Opti-FDTD Simulation, Photonic Bandgap Structures

INTRODUCTION
The advent of random lasers has introduced a paradigm shift in the field of photonics, leveraging light amplification through multiple scattering in disordered gain media (Silva et al., 2024). Unlike conventional lasers that rely on well-defined cavities, random lasers operate without mirrors or resonant cavities, offering unique advantages such as compactness, isotropic emission, and tuneable spectral properties (Han, et al., 2024). Despite their significant potential, optimizing random laser performance remains a challenge due to the inherent complexity of disordered media. Scatterer distribution plays a pivotal role in shaping the dynamics of light-matter interaction, directly influencing emission characteristics (Cheng et al., 2024). This research seeks to address this complexity by employing advanced computational modelling to investigate the effect of scatterer distribution on random laser behaviour.

Overview of Random Lasers
Random lasers operate based on the principles of light scattering and amplification (Abass, Jawad, Haider, & Taha, 2024). In these systems, gain materials embedded in disordered structures provide the necessary feedback for light amplification through multiple scattering paths (Zhu, et al., 2024). The absence of a defined optical cavity results in unique spectral and spatial emission properties (Moon et al., 2024), making random lasers suitable for diverse applications, including biomedical imaging, sensing, and spectroscopy (Ni et al., 2022). However, the performance of random lasers is highly sensitive to the spatial arrangement and density of scatterers within the medium (Padiyakkuth et al., 2022) which necessitates a comprehensive understanding of their impact on key laser parameters.

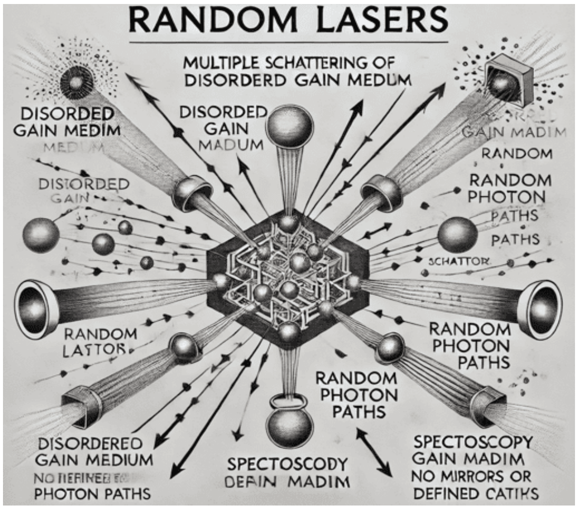

Figure 1: The key concepts of Introduction to Random lasers

Figure 1, describes how light is amplified through multiple scattering in a disordered gain medium, Bypassing the need for Mirrors or a defined cavity. Instead, photons follow random paths, enabling lasing. This unique mechanism supports applications in imaging, spectroscopy, and lighting.

Role of Scatterer Distribution in Enhancing Random Laser Performance

The distribution of scatterers within the gain medium critically determines the feedback mechanism and emission efficiency of random lasers (Moura et al., 2023). Low-density scatterer configurations may result in weak feedback and broad emission spectra (Yang et al., 2024), while high-density distributions can lead to excessive scattering losses and suppressed laser action (Chen et al., 2023). An optimal distribution enhances light confinement, achieving balanced feedback and high emission efficiency (Du et al., 2021). Investigating this interplay requires robust simulation tools capable of capturing the complex interactions between scatterers and electromagnetic fields. This study utilizes the Opti-FDTD simulation platform to systematically explore the impact of varying scatterer densities and configurations on random laser performance.

Despite extensive research, the precise mechanisms by which scatterer distribution influences random laser characteristics remain poorly understood, primarily due to the challenges associated with modelling highly disordered systems. This research aims to bridge this gap by employing Opti-FDTD simulations to analyse the effect of scatterer distribution on the emission properties of random lasers.

Basic Principles of Random Lasers

Random lasers represent a unique class of optical devices that operate without the conventional resonant cavity (Abdulhameed, 2024), relying instead on disordered media to provide the necessary feedback for lasing action. The fundamental principle underlying random lasers is the amplification of light through stimulated emission within a scattering medium (Lippi, 2021). In these systems, gain materials, such as doped glass or polymers, are embedded in a matrix with randomly distributed scatterers (Vasconcelos et al., 2025). The random arrangement of scatterers causes multiple scattering events, creating random optical feedback paths that enhance light-matter interaction (Simon et al., 2024). This feedback mechanism, coupled with sufficient gain, leads to lasing action characterized by unique emission spectra and spatial coherence properties (Carvalho et al., 2025). Random lasers are highly versatile, and hold promise for applications in imaging, sensing, and spectroscopy (Ahmad et al., 2025).

Mechanisms of Light Amplification via Multiple Scattering

The lasing process in random lasers is governed by the interaction between light and scatterers within the medium (Dey et al., 2025). Light entering the disordered structure undergoes multiple scattering events, leading to the creation of random optical paths (Meglinski et al., 2024). In the presence of an optical gain medium, photons traveling along these random paths stimulate the emission of additional photons with the same frequency and phase (Lu et al., 2024). This results in the exponential amplification of light intensity along certain paths. Unlike conventional lasers, where feedback is achieved through cavity mirrors, random lasers depend on scattering-induced feedback (Aurelio et al., 2025), which can vary based on the density and spatial distribution of scatterers. The strength of this feedback determines key laser parameters, such as threshold, emission spectrum, and spatial coherence. A well-engineered scatterer configuration can enhance feedback efficiency, reduce the lasing threshold, and optimize overall performance.

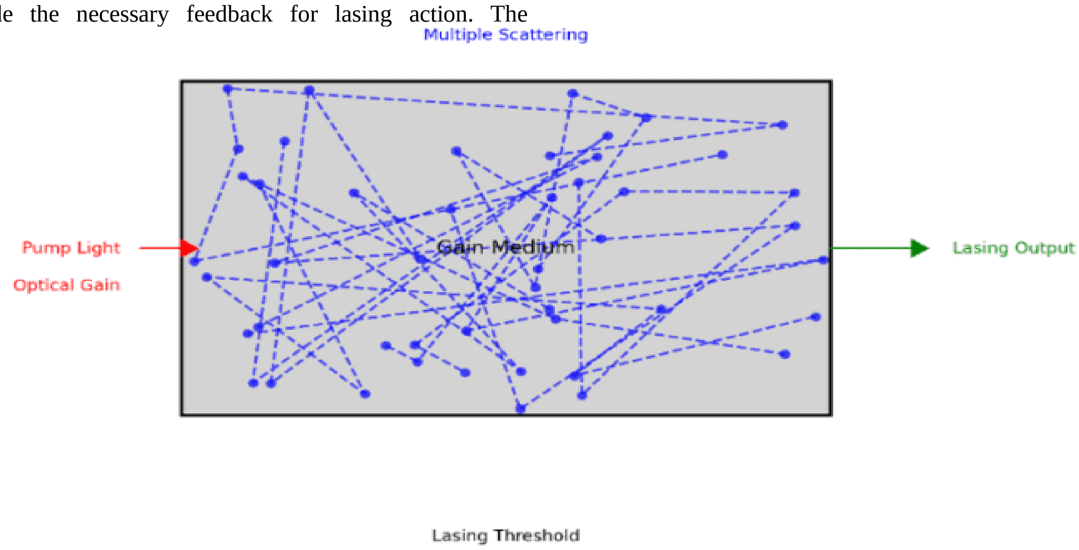

Figure 2: Diagram illustrating the basic principles and mechanisms of random lasers

As shown in Figure 2, light undergoes numerous scattering events within a disordered gain medium. The gain medium amplifies light to counteract scattering and absorption losses (Kadhim et al., 2025), and lasing is achieved when optical gain surpasses these losses, resulting in coherent light emission.

Introduction to Photonic Band Gap (PBG) Structures

Photonic Band Gap (PBG) structures play a pivotal role in enhancing random laser performance by providing controlled light confinement and feedback mechanisms (Gangwar et al., 2023). PBG structures are periodic arrangements of materials with alternating refractive indices, designed to inhibit the propagation of certain wavelengths of light within specific frequency ranges, known as band gaps (Miyan et al., 2023). When combined with random scattering media, PBG structures can manipulate light propagation, effectively enhancing feedback for lasing action (Hayat et al., 2024). The integration of PBG structures into random laser systems offers several advantages, including improved spectral control, reduced scattering losses, and enhanced spatial coherence. By designing PBG structures with tailored periodicity and geometry (Wang et al., 2023), it is possible to achieve precise control over light-matter interactions, paving the way for the development of high-efficiency random lasers.

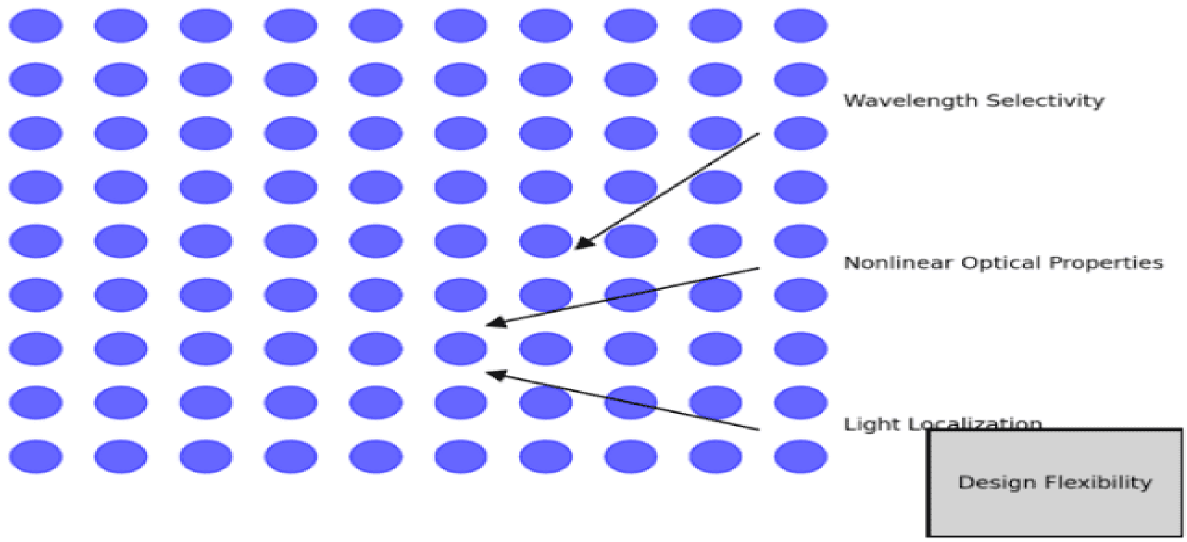

Figure 3: Diagram illustrating the key characteristics of Photonic Band Gap (PBG) structures

Figure 3, describes how the Photonic band gap structures provide wavelength selectivity, nonlinear optics, and enhanced light confinement, boosting efficiency, controlled emission, and output power in random lasers.

MATERIALS AND METHODS

The Optical Finite-Difference Time-Domain (Opti-FDTD) software serves as the primary simulation tool for this research, providing advanced capabilities for modelling and analysing photonic structures, including photonic bandgap (PBG) materials and waveguides (Geerthana et al., 2023). To construct the simulation environment, high-purity silica (SiO_2) is used as the background material due to its excellent optical transparency and low loss characteristics, while zinc oxide (ZnO) scatterers are introduced to create disorder and enable multiple scattering effects. Opti-FDTD facilitates the detailed exploration of electromagnetic wave propagation, allowing for the design and optimization of PBG structures with varying scatterer distributions. Its ability to simulate both 2D and 3D photonic systems makes it a powerful tool for examining the complex interactions within random laser models, particularly in studying lasing thresholds, emission spectra, and spatial coherence under different scatterer densities.

Design and Simulation of PBG Structures

The study focuses on designing PBG structures tailored to investigate the effect of scatterer distribution on random laser performance.

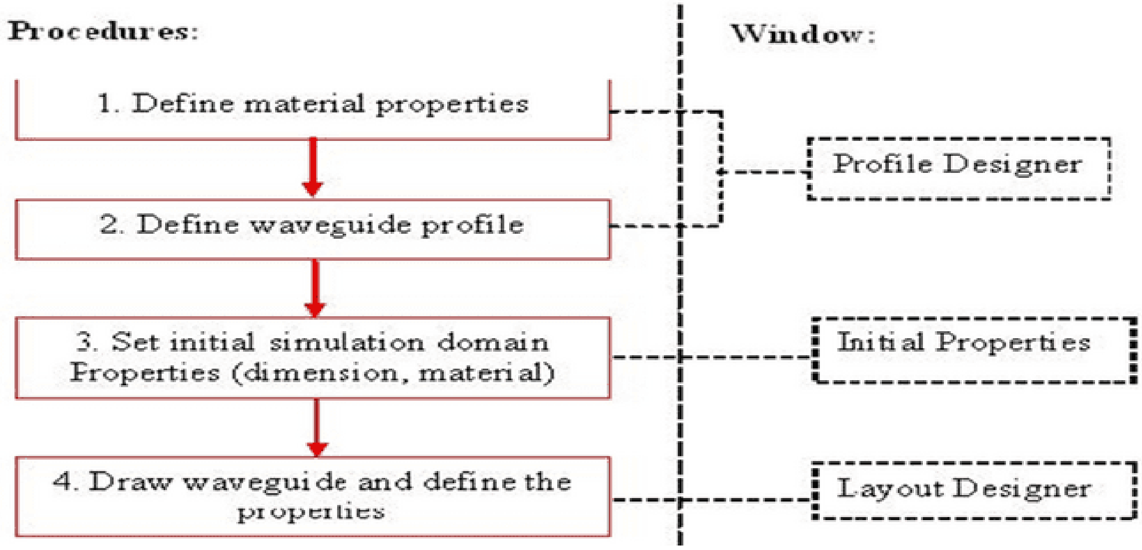

Figure 4: Flow chart showing the Designing Processes

Figure 4 outlines the essential steps in the design process for analysing scatterer distribution effects on a random laser model using Opti-FDTD software. It begins by defining the material properties in the "Profile Designer" window, proceeds to specifying the waveguide profile, and then establishes the initial simulation domain's dimensions and materials in the "Initial Properties" window. Finally, the process involves drawing the waveguide and detailing its properties within the "Layout Designer" window.

Designing a PBG structure

A new project for designing a PBG structure was initiated in Waveguide Layout Designer. A new dielectric material, named "PBG atom" with a refractive index of 3.1, was defined within the Profile Designer (Geerthana et al., 2023).

Defining the Channel Profile

In Opti-FDTD Designer, under the Profiles folder, a new channel profile (Profile PBG) was created via the Channel folder. Specifications included: 2D profile (Material: PBG atom) and 3D profile (Layer name: layer_01, Width: 1.0, Thickness: 1.0, Offset: 0.0, Material: PBG atom). The material was saved (Store), and Profile Designer was closed.

Defining the wafer and waveguide properties

In the Initial Properties dialog, Default Waveguide Width: 1.0 µm, Profile: Profile PBG, Wafer Dimensions: Length 21.0 µm, Width 15.0 µm. 2D Wafer Material: Air. 3D Wafer Properties: Cladding and Substrate Material: Air, Thickness: 1.0 µm each. Closed dialog with OK

Creating the PBG structure

From the Draw menu, the PBG Crystal Structure was created and edited in the layout window (Figure 4(b)). Key parameters: Origin Offset (Horizontal: 1.0, Vertical: -6.928), Depth: 0.0, Azimuth: 0.0, 2D Hexagonal Lattice, Fill: Block, Dimensions (Scale: 1.0, #A: 17, #C: 19), Label: PBG Crystal Struct1. Dialog remained open.

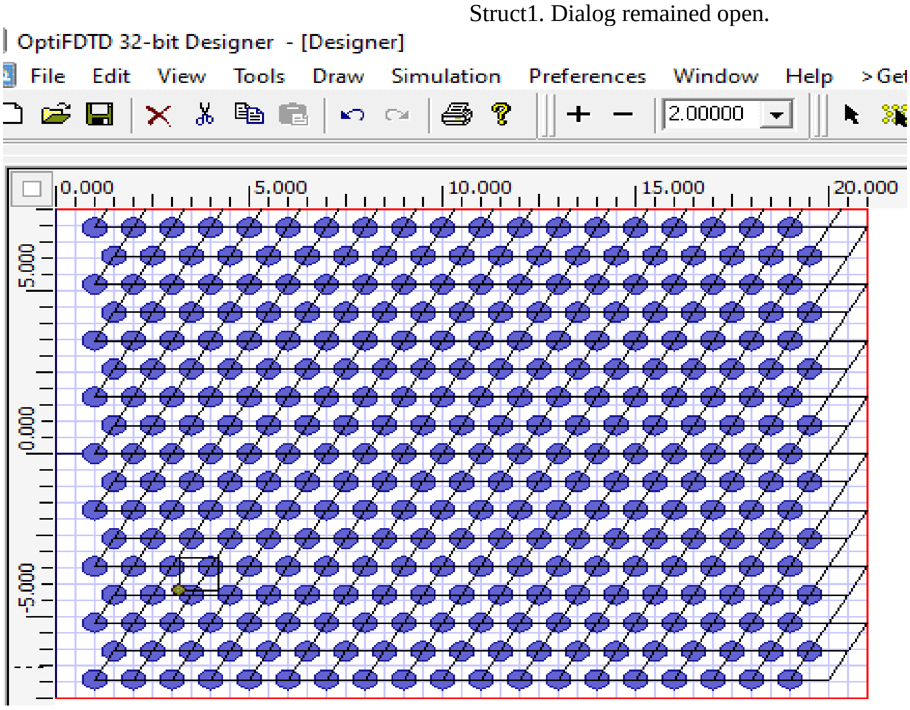

Figure 4 (b): PBG structure in layout window

Setting the atom properties

An elliptic waveguide labelled "Atom" with Profile: Profile PBG was added in the Atom Waveguide in Unit Cell. Key parameters included center offsets (horizontal and vertical: 0.0), major and minor radii (0.3), orientation angle (0.0), depth (0.0), and default channel tapering.

Creating a cell for Scatterer Distribution

The scatterer distribution was applied to a selected PBG structure, adjusting position, size, and density to ensure proper integration within the layout.

Inserting the input plane

A Vertical Input Plane was added with wavelength: 1.9 µm (optimized for low attenuation). Gaussian Modulated CW parameters included time offset: 5.5e-14 s, half-width: 1.1e-14 s, transverse Gaussian input with center: 0.0 µm, half-width: 0.8 µm, and amplitude: 1.0 V/m. Plane geometry was configured with Z position: 1.3 µm and positive direction.

Setting up the Observation Point

Observation points labelled Observation Point1, Point2, and Point3 were positioned at (19.5 µm, 4.33 µm), (19.5 µm, -4.33 µm), and (0.8 µm, 0.0 µm), respectively, with a center depth of 0.0 µm. All monitored 2D TE: Ey field components for accurate data collection.

Setting the 2D TE FDTD simulation parameters

Simulation settings included TE polarization, mesh size (ΔX, ΔY: 0.1 µm), and Anisotropic PML boundaries with specified parameters. Time steps were set to 10,000, with Input Plane1 at a wavelength of 1.9 µm.

Observing the simulation results in Opti-FDTD Simulator

The Opti-FDTD Simulator displayed refractive index distribution and wave propagation, with dynamic time and frequency domain responses observed at defined observation points.

Simulation Parameters and Observation Metrics

To simulate the interaction of light with the designed PBG structures, the Transverse Electric (TE) mode is selected to focus on the electric field component perpendicular to the propagation direction. A fine spatial and temporal mesh resolution is employed to capture detailed variations in the electromagnetic field. Light entering the medium is modelled using a Gaussian-modulated continuous wave with a wavelength of 1.9 µm. Strategic observation points are configured to monitor field propagation, transmission, and reflection characteristics. Key metrics, including the lasing threshold, emission spectrum, and spatial coherence, provide valuable insights into the role of scatterer distribution in random laser performance.

RESULTS AND DISCUSSION

Results

The lasing threshold, emission spectrum, spatial coherence, and light localization were significantly influenced by the scatterer density. In the low-density configuration, widely spaced scatterers resulted in weak optical feedback and high energy losses, leading to a high lasing threshold, broad and less defined emission spectrum, poor spatial coherence, and weak light localization due to diffuse and unconfined emission

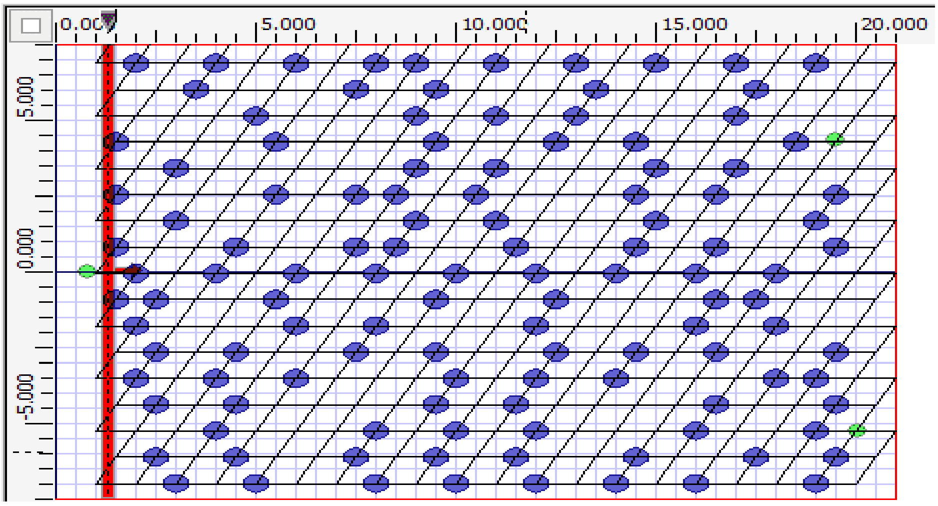

Figure 5: Atomic Spacing in Low-Density Photonic Band Gap (PBG) Materials

Figure 5 (a) shows a smoother refractive index distribution with larger atomic spacing, reducing contrast and broadening photonic bandgaps, affecting light propagation control.

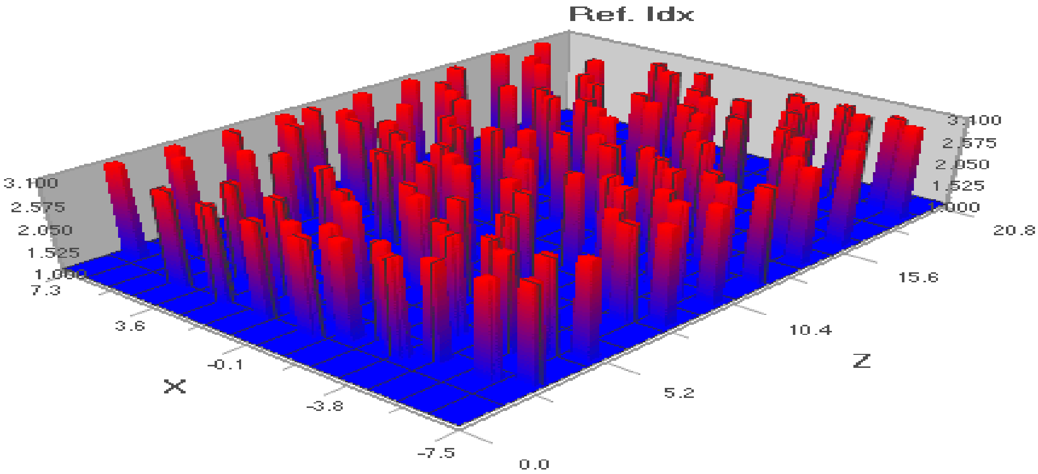

Figure 5 (a): The Refractive index Structure for a Low-Density PBG Materials

Figure 5 (b) shows DFT analysis with reduced intensity, weaker confinement, and diminished field strength due to low-density atom spacing, limiting magnetic field coupling and resonance.

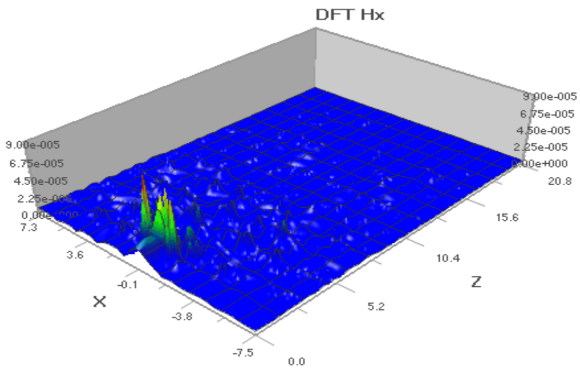

(i) DFT Hx

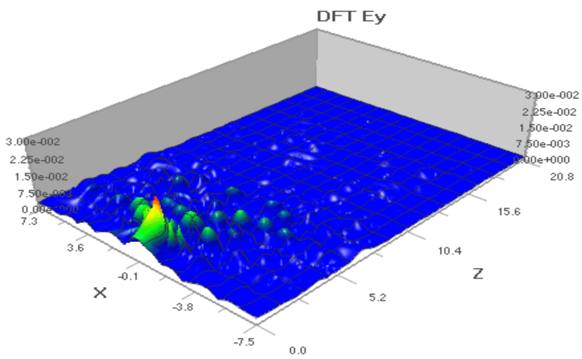

(ii) DFT Ey

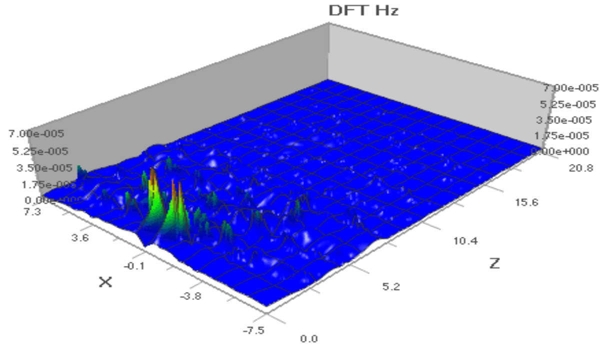

(iii) DFT Hz

Figure 5 (b) Discrete Fourier Transform (DFT) for (i) the electric field in y-direction, (ii) magnetic field component in x-direction, and (iii) magnetic field component in z-direction for a Low-Density PBG Materials

Figure 5 (c) shows smoother energy flow with reduced scattering and diffraction due to increased spacing, enhancing transmission efficiency.

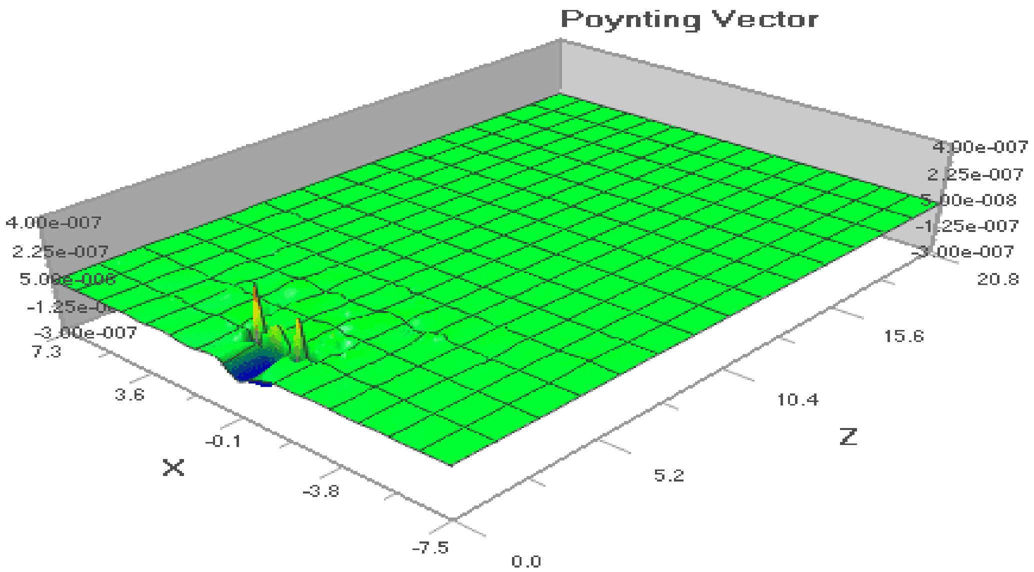

Figure 5 (c) Poynting vector for a Low-Density PBG Materials

Figure 5 (d) shows clearer transmission and reflection at Observation Points 1 and 2, with reduced scattering and improved resonance isolation due to wider atomic spacing.

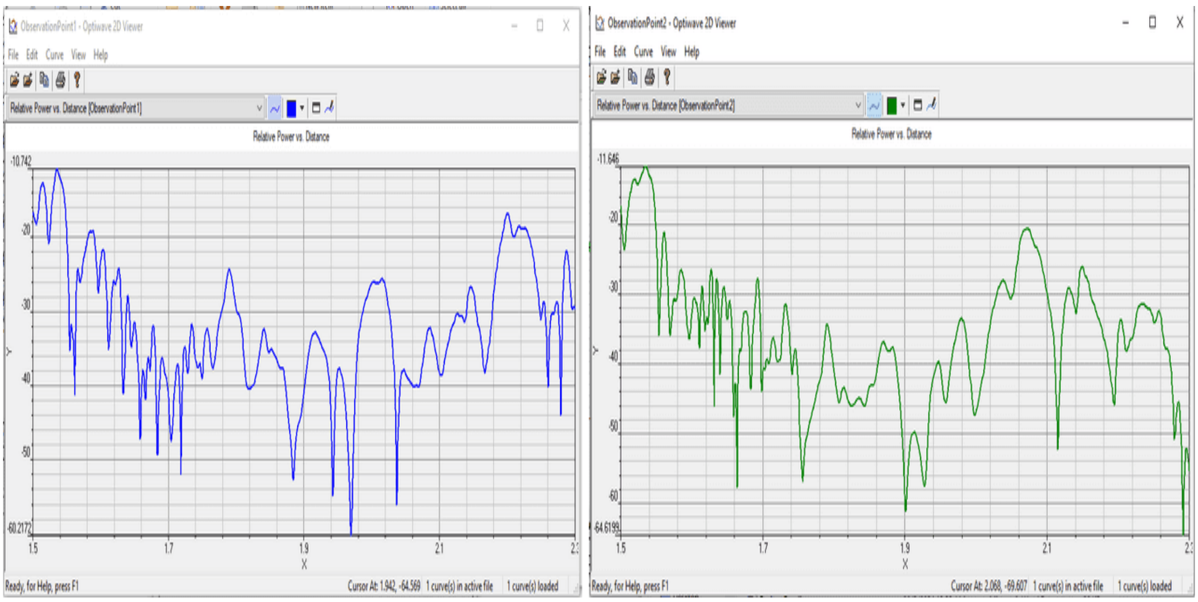

Figure 5 (d) Observation Area Analysis (1 and 2) for a Low-Density PBG Materials

Conversely, the medium-density configuration, with balanced scatterer spacing, exhibited the lowest lasing threshold, sharp and well-defined spectral peaks, enhanced spatial coherence, and strong light localization due to optimal feedback and confinement.

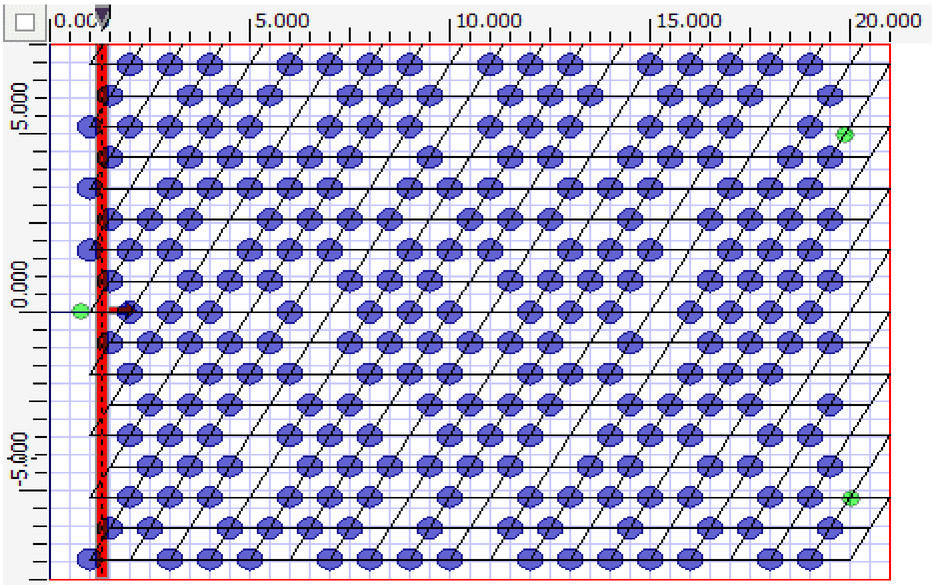

Figure 6: Atomic Spacing in Medium-Density Photonic Band Gap (PBG) Materials

Figure 6 (a) shows a clear refractive index contrast, defining an optimal photonic bandgap for effective light confinement and guided modes.

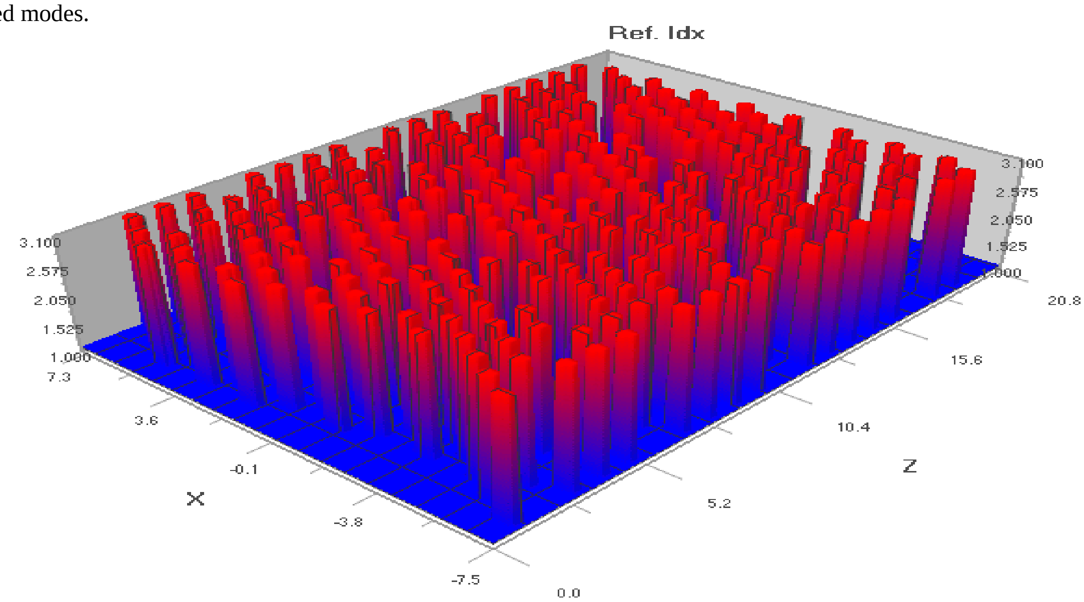

Figure 6 (a): Refractive index for a Medium-Density PBG Materials

Figure 6 (b) shows DFT Hx, Ey, and Hz with moderate confinement, efficient coupling, and strong resonances, indicating effective interaction with the PBG structure.

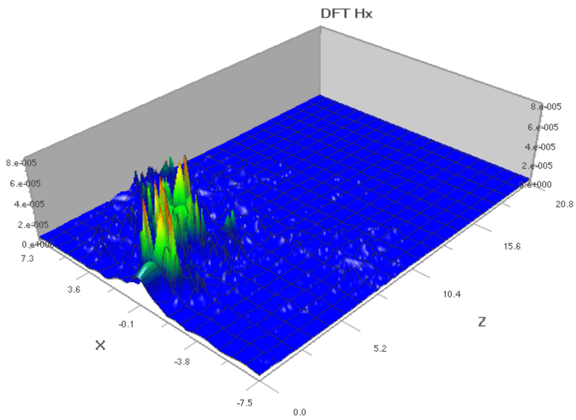

(i) DFT Hx

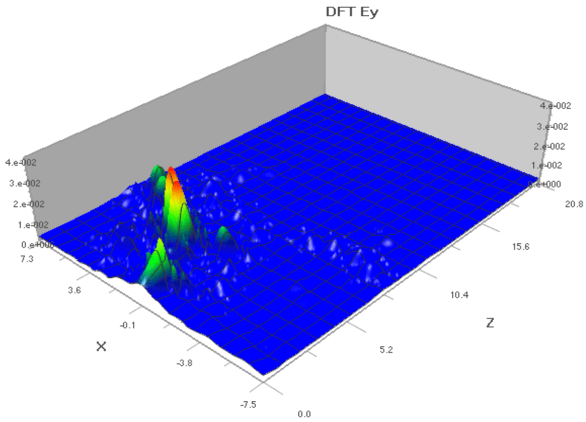

(ii) DFT Ey

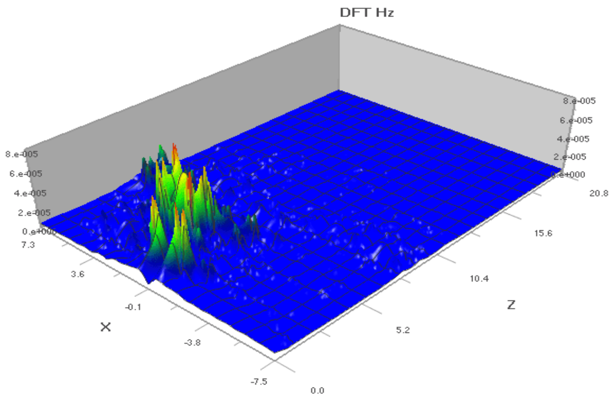

(iii) DFT Hz

Figure 6 (b) Discrete Fourier Transform (DFT) for (i) the electric field in y-direction, (ii) magnetic field component in x-direction, and (iii) magnetic field component in z-direction for a Medium-Density PBG Materials

Figure 6 (c) shows balanced energy flow with moderate scattering and smooth propagation, ensuring efficient energy transfer.

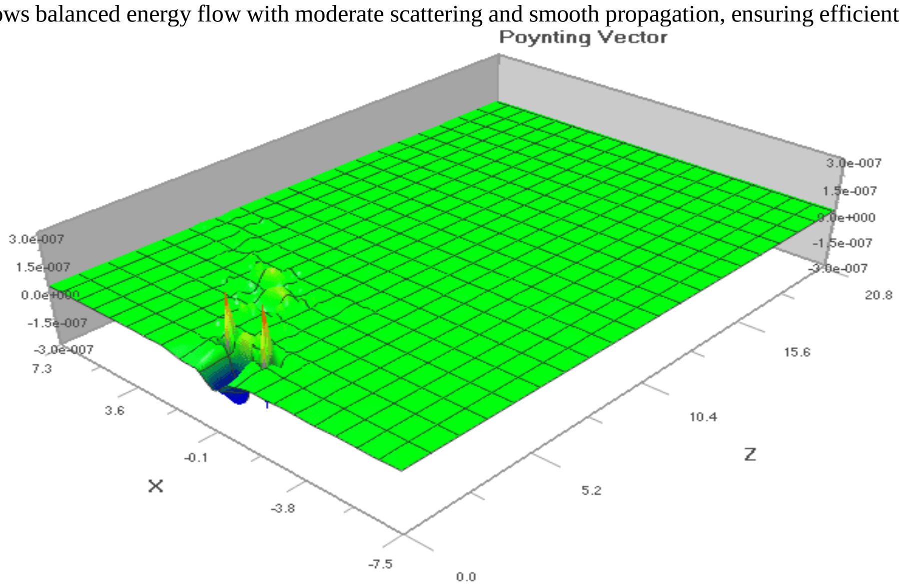

Figure 6 (c): Poynting Vector for a Medium-Density PBG Materials

Figure 6 (d) shows clear transmission and reflection at Observation Points 1 and 2, with well-defined peaks and a balanced photonic bandgap.

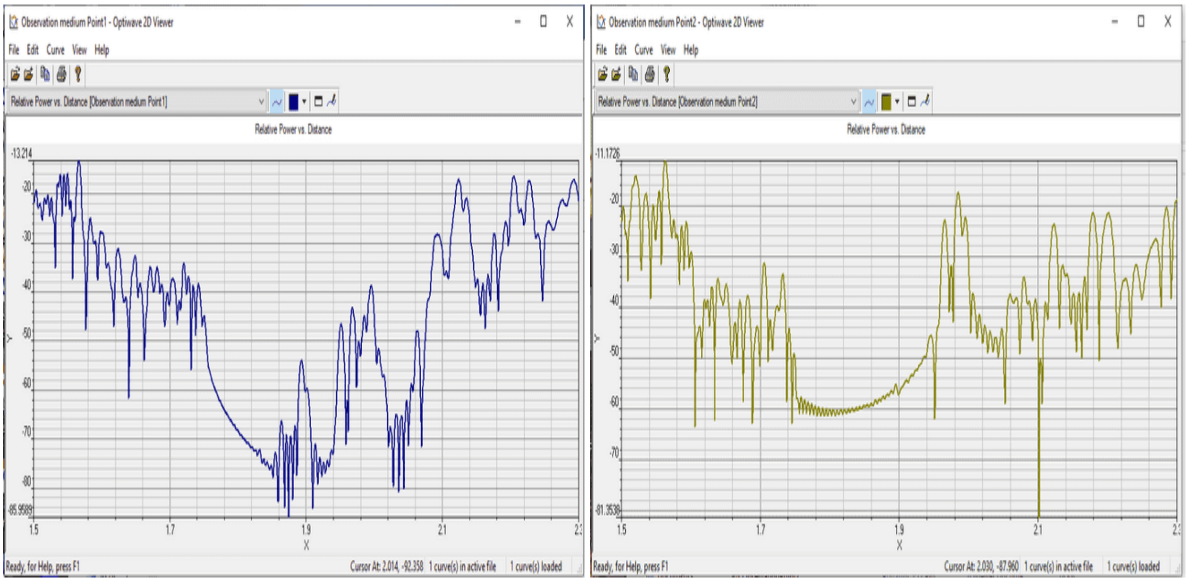

Figure 6 (d): Observation Area Analysis (1 and 2) for a Medium-Density PBG Materials

While the high-density configuration offered strong scattering feedback, excessive density introduced significant scattering losses, resulting in a higher lasing threshold than the medium-density case, intense but overlapping spectral peaks, and reduced spatial coherence despite strong light localization.

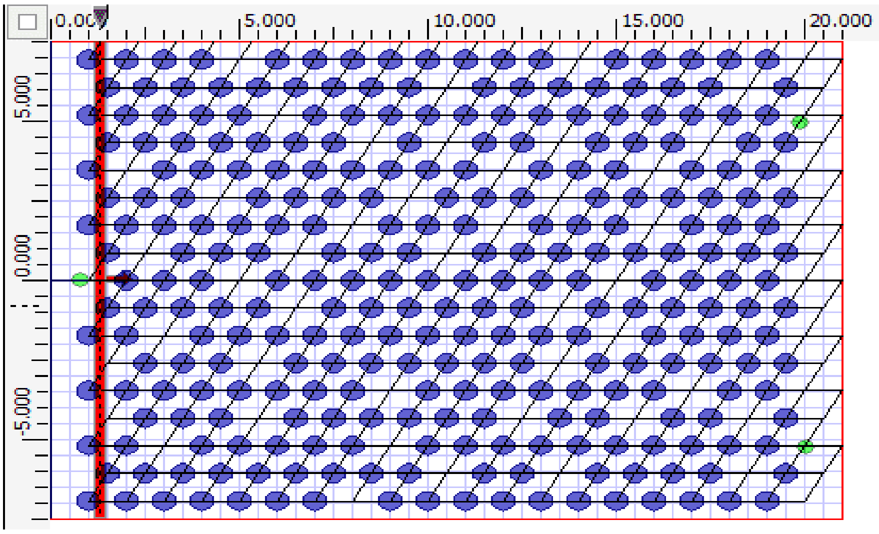

Figure 7: Atomic Spacing in a High-Density Photonic Band Gap (PBG) Materials

Figure 7 (a) shows sharp refractive index contrasts, defining the photonic bandgap. Tightly packed atoms enhance periodicity, improving light confinement and guiding.

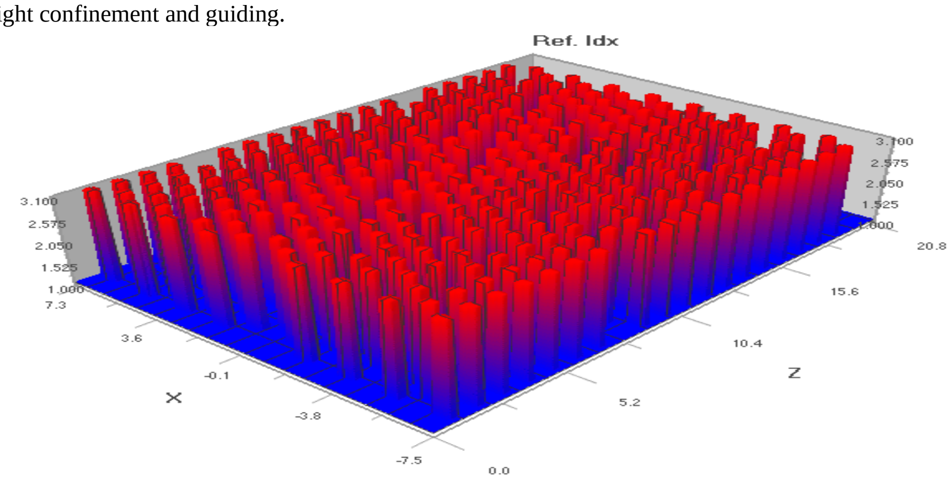

Figure 7 (a): The Refractive index Structure for a High-Density PBG Materials

Figure 7 (b) shows DFT Hx, Ey, and Hz exhibit strong periodicity, field confinement, and resonances, highlighting effective interaction and coupling with the dense structure.

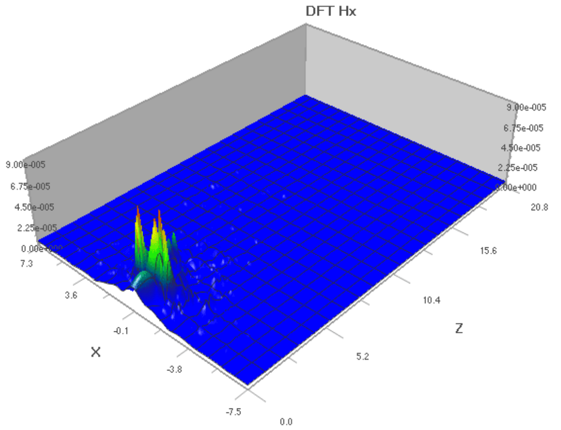

(i) DFT Hx

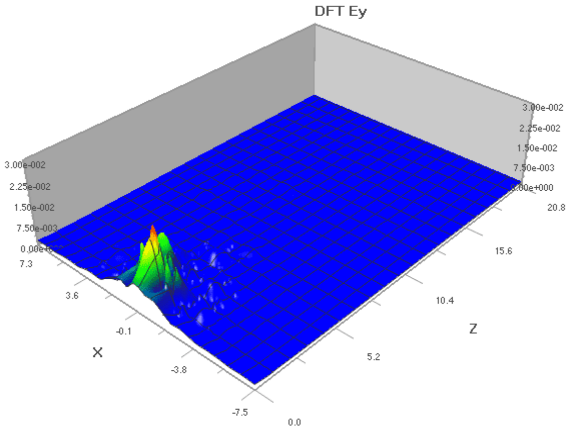

(ii) DFT Ey

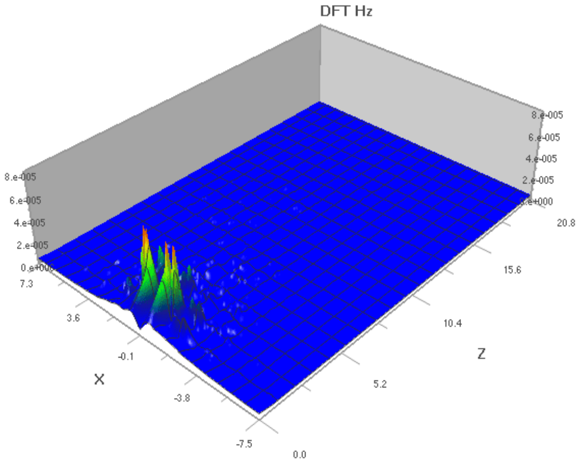

(iii) DFT Hz

Figure 7 (b): Discrete Fourier Transform (DFT) for (i) the electric field in y-direction, (ii) magnetic field component in x-direction, and (iii) magnetic field component in z-direction for a High-Density PBG Materials

Figure 7 (c) shows localized energy flow with increased scattering and disruptions due to densely packed atoms.

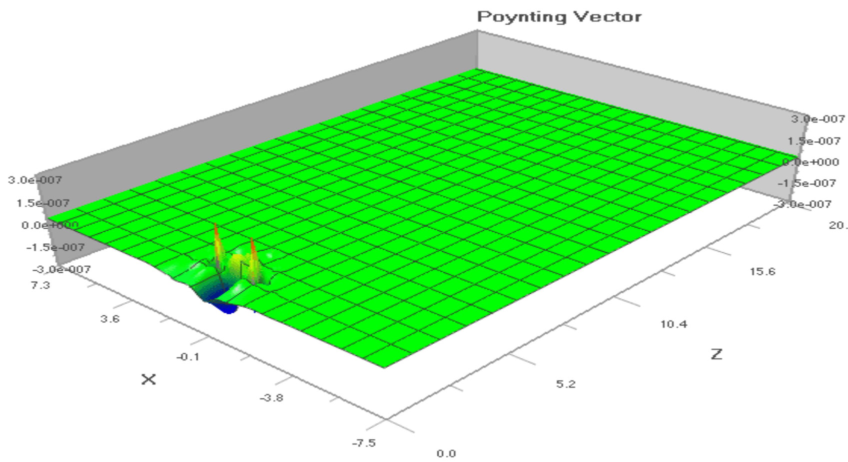

Figure 7 (c): Poynting Vector for a High-Density PBG Materials

Figure 7 (d) shows sharp peaks and dips in transmission and reflection at Observation Points 1 and 2, highlighting strong scattering and a pronounced photonic bandgap.

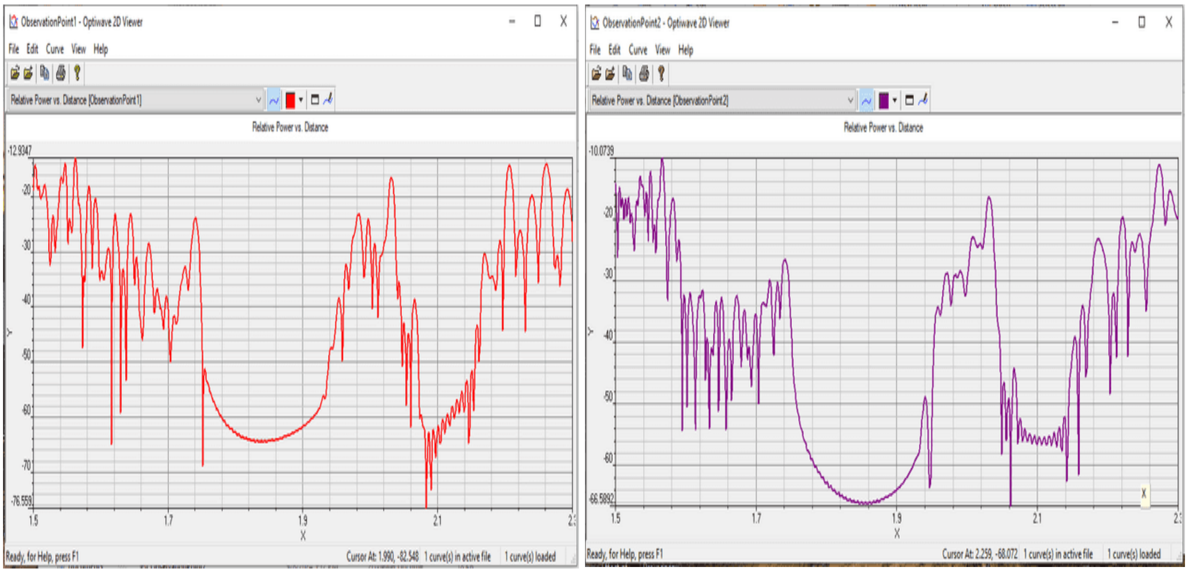

Figure 7 (d): Observation Area Analysis (1 and 2) for a High-Density PBG Materials

Discussion

The lasing threshold, emission spectrum, spatial coherence, and light localization are significantly influenced by scatterer density, as documented in various studies. In low-density configurations, widely spaced scatterers lead to weak optical feedback and high energy losses, resulting in a high lasing threshold, broad and less defined emission spectrum, poor spatial coherence, and weak light localization due to diffuse and unconfined emission. These observations are consistent with findings reported in the FUDMA Journal of Sciences, where similar behaviours have been noted in photonic systems with varying scatterer densities. For instance, (Ivan et al., 2017), demonstrated that increased scatterer density enhances optical confinement and coherence, leading to improved laser performance. Therefore, our results reinforce the understanding that scatterer distribution plays a crucial role in tuning random laser performance for practical applications.

Comparison with Theoretical and Experimental Models

The results align closely with theoretical predictions and experimental findings:

The lasing threshold trends match established theories, with medium-density configurations providing the most efficient lasing performance.

The emission spectrum characteristics corroborate experimental data, showing narrower and higher-intensity peaks for medium-density scatterers.

Spatial coherence results confirm prior models, demonstrating that medium-density distributions offer the best trade-off between light localization and phase uniformity.

CONCLUSION

These findings highlight the critical role of medium to high-density PBG atom arrangements in achieving desired spatial coherence and consistent optical behaviour in random laser applications, offering practical advantages for advanced photonic devices. Future research should incorporate extended simulations to explore additional variables such as scatterer refractive index and nonlinear optical interactions, while experimental validation and investigations across a broader spectral range with novel scatterer materials could further enhance performance and applicability.

REFERENCES

Abass, N. A., Jawad, M. F., Haider, A. J., & Taha, B. A. (2024). Exploring random laser characteristics in core@ shell nano-scatter centers: trends and opportunities. *Optical and Quantum Electronics, 56(12)*, https://doi.org/10.1007/s11082-024-06881-y

Abdulhameed, A. (2024). ZnO-based random lasing and their sensing applications: a mini-review. *Applied Nanoscience, 14(10)*, 985-995. http://dx.doi.org/10.1007/s13204-024-03059-6

Ahmad, A., Dai, H. T., Feng, S., Chen, Z., Mohamed, Z., Khan, A. A., & Mehvish, D. (2025). Random lasing in liquid crystal: Advances, Challenges, and Future Directions. *Journal of Materials Chemistry C.* https://pubs.rsc.org/en/content/articlelanding/2025/tc/d4tc04871g

Aurelio Sarabia-Alonso, J., Vidales Pasos, E., Belamkar, A., Wagner, B., & Mangolini, L. (2025). Titanium nitride nanoparticles as plasmonic nanothermometers. *Optics Express, 33(4)*, 6758-6770. http://dx.doi.org/10.1364/OE.549815

Carvalho, A. J., Gonçalves, I. M., Santos, E. P., Pincheira, P. I., Araujo, P. M., de Oliveira, H. P., & Gomes, A. S. (2025). Dye-doped electrospun fiber-based random lasers: The influence of combined gain media. *Optical Materials*, *159*, 116647. https://doi.org/10.1016/j.optmat.2025.116647

Chen, M. H., Xing, D., Su, V. C., Lee, Y. C., Ho, Y. L., & Delaunay, J. J. (2023). GaN ultraviolet laser based on bound states in the continuum (BIC). *Advanced Optical Materials, 11(6)*, 2201906. https://doi.org/10.1002/adom.202201906

Cheng, M. J., Cao, Y. C., Ren, K. F., Zhang, H., & Guo, L. X. (2024). Generalized Lorenz-Mie theory and simulation software for structured light scattering by particles. *Frontiers in Physics, 12*, 1354223. https://www.frontiersin.org/journals/physics/articles/10.3389/fphy.2024.1354223/full

Dey, A., Pramanik, A., Karmakar, S., Biswas, S., Karthikeyan, J., Messina, F., & Kumbhakar, P. (2025). Black TiO2 Nanoparticles as Plasmonically Active Scatterers for Random Lasing. *ACS Applied Nano Materials*. https://pubs.acs.org/doi/10.1021/acsanm.4c07082

Du, P., Li, J., Wang, L., Sun, L., Wang, X., Xu, X., & Tang, J. (2021). Efficient and large-area all vacuum-deposited perovskite light-emitting diodes via spatial confinement. *Nature Communications, 12(1)*, 4751. https://www.nature.com/articles/s41467-021-25093-6

Gangwar, R. K., Pathak, A. K., & Kumar, S. (2023). October). Recent progress in photonic crystal devices and their applications. *a review. In Photonics (Vol. 10, No. 11*, p. 1199). MDPI. https://www.mdpi.com/2304-6732/10/11/1199

Geerthana, S., Sridarshini, T., Syedakbar, S., Nithya, S., Balaji, V. R., Thirumurugan, A., & Dhanabalan, S. S. (2023). A novel 2D-PhC based ring resonator design with flexible structural defects for CWDM applications. *Physica Scripta, 98(10)*, 105975. https://doi.org/10.1088/1402-4896/acfa43

Han, B., Cheng, Q., Tao, Y., Ma, Y., Liang, H., & Ma, R. .. (2024). Spectral manipulations of random fiber lasers: principles, characteristics, and applications. *Laser & Photonics Reviews, 18(7)*, 2400122. https://onlinelibrary.wiley.com/doi/abs/10.1002/lpor.202400122

Hayat, A., Jin, Y., Iqbal, N., Zhai, T., & He, S. (2024). Lasers Based on Periodic and Quasiperiodic Planar Feedback Cavities: Designs, Principle, and Potential Applications. *Progress in Electromagnetics Research*, 126. DOI: http://dx.doi.org/10.2528/PIERM24013106

Iván R. Roa González, Bismarck C. Lima, Pablo I. R. Pincheira, Arthur A. Brum, Antônio M. S. Macêdo, Giovani L. Vasconcelos, Leonardo de S. Menezes, Ernesto P. Raposo, Anderson S. L. Gomes, Raman Kashyap (2017). Turbulence Hierarchy in a Random Fibre Laser. https://doi.org/10.48550/arXiv.1707.00946

Kadhim, N. M., Vahed, H., & Soofi, H. (2025). Electrically Pumping of SOI Metamaterial Gain-Stripes Plasmonic Nanolaser with DBR Structure. *Plasmonics*, 1-28. http://dx.doi.org/10.1007/s11468-024-02700-y

Lippi, G. L. (2021). Amplified Spontaneous Emission" in Micro- and Nanolasers. *Atoms, 9(1)*, 6. https://www.mdpi.com/2218-2004/9/1/6

Lu, H., Alkhazragi, O., Wang, Y., Almaymoni, N., Yan, W., Gunawan, W. H., & Ooi, B. S. (2024). Low-coherence semiconductor light sources: devices and applications. *npj Nanophotonics*, *1(1)*, 9. https://www.nature.com/articles/s44310-024-00005-w

Meglinski, I., Lopushenko, I., Sdobnov, A., & Bykov, A. (2024). Phase preservation of orbital angular momentum of light in multiple scattering environment. *Light: Science & Applications, 13(1)*, 214. https://www.nature.com/articles/s41377-024-01562-7

Miyan, H., Agrahari, R., Gowre, S. K., Jain, P. K., & Mahto, M. (2023). Photonic crystal based ultrafast and highly sensitive refractive index sensor. *IEEE Sensors Journal*, *23(14)*, 15563-15569. DOI: http://dx.doi.org/10.1109/JSEN.2023.3283506

Moon, J., Mehta, Y., Gundogdu, K., So, F., & Gu, Q. (2024). Metal-halide perovskite lasers: Cavity formation and emission characteristics. *Advanced Materials, 36(20)*, 2211284. https://doi.org/10.1002/adma.202211284

Moura, A. L., Pincheira, P. I., de Araújo, C. B., & Gomes, A. S. (2023). Feedback Mechanisms and Modes of Random Lasers. In Lévy Statistics and Spin Glass Behavior in Random Lasers. *Jenny Stanford Publishing*, (pp. 23-50). https://www.taylorfrancis.com/chapters/edit/10.1201/9781003336181-2/feedback-mechanisms-modes-random-lasers-andr%C3%A9-moura-pablo-pincheira-cid-de-ara%C3%BAjo-anderson-gomes

Ni, D., Späth, M., Klämpfl, F., & Hohmann, M. (2022). Properties and applications of random lasers as emerging light sources and optical sensors: a review. *Sensors, 23(1)*, 247. ; https://doi.org/10.3390/s23010247

Padiyakkuth, N., Thomas, S., Antoine, R., & Kalarikkal, N. (2022). Recent progress and prospects of random lasers using advanced materials. *Materials Advances, 3(17)*, 6687-6706. https://pubs.rsc.org/en/content/articlelanding/2022/ma/d2ma00221c

Silva, L. A., Ferreira, F. S., Oliveira, G. S., Moura, A. L., de Oliveira, R. A., & Reyna, A. S. (2024). Exploring disordered light transport in scattering media to optimize random lasers. *The Journal of Physical Chemistry C, 128(12)*, 5321-5329. https://scholar.google.com.my/citations?user=be52EiEAAAAJ&hl=el

Simon, A., Baudis, Q., Wunenburger, R., & Valier-Brasier, T. (2024). Propagation of elastic waves in correlated dispersions of resonant scatterers. *The Journal of the Acoustical Society of America, 155(6)*, 3627-3638. https://doi.org/10.1121/10.0026233

Vasconcelos, H. C., Meirelles, M., Özmenteş, R., & Santos, L. (2025). Structural Analysis of Erbium-Doped Silica-Based Glass-Ceramics Using Anomalous and Small-Angle X-Ray Scattering. *Foundations, 5(1)*, 5. https://doi.org/10.3390/foundations5010005

Wang, Y., Gong, C., Yang, X., Zhu, T., Zhang, K., Rao, Y. J., & Gong, Y. (2023). Photonic Bandgap Fiber Microlaser with Dual-Band Emission for Integrated Optical Tagging and Sensing. *Laser & Photonics Reviews, 17(6)*, 2200834. DOI: http://dx.doi.org/10.1002/lpor.202200834

Yang, Q., Wu, Y., Chen, J., Lu, M., Wang, X., Zhang, Z., & Chen, L. (2024). Plasmonic nanomaterial-enhanced fluorescence and Raman sensors: Multifunctional platforms and applications. *Coordination Chemistry Reviews, 507*, 215768. https://doi.org/10.1016/j.ccr.2024.215768

Zhu, H., He, Z., Wang, J., Zhang, W., Pei, C., Ma, R., & Liu, W. (2024). Microcavity complex lasers: From order to disorder. *Annalen der Physik, 536(9)*, 2400112. https://doi.org/10.1002/andp.202400112